

# Remazol red dye removal using poly(acrylamide-*co*-acrylic acid) hydrogels and water absorbency studies

Miguel A. Corona-Rivera<sup>1</sup> · Víctor M. Ovando-Medina<sup>1</sup> · Luis A. Bernal-Jacome<sup>2</sup> · Elsa Cervantes-González<sup>1</sup> · Iveth D. Antonio-Carmona<sup>1</sup> · Nancy E. Dávila-Guzmán<sup>3</sup>

Received: 22 March 2016 / Revised: 5 December 2016 / Accepted: 6 December 2016 / Published online: 16 December 2016  
© Springer-Verlag Berlin Heidelberg 2016

**Abstract** Acrylamide (AAM) and acrylic acid (AAc) were copolymerized in aqueous solution using 2,2-azobis(2-amidinopropane) hydrochloride (V-50) as initiator and *N,N'*-methylenebisacrylamide (NMBAM) as cross-linking agent to obtain high swelling hydrogels. The effects of AAM/AAc ratio and the amount of cross-linking agent on the swelling properties were studied. It was observed that swelling characteristics of hydrogels are highly affected by the presence of carboxylic groups of AAc units in the hydrogels and by the cross-linking amount in the polymer chains. Hydrogel with 70/30 ratio of AAM/AAc showed the highest swelling degree, until 69.2 g of water/g of dried hydrogel, which represents approximately 7000% of swelling. Swelling kinetic was well represented by a second-order kinetic model for all the AAM/AAc compositions with maximum weight swelling ratio

between 20.4 and 82.6 g/g for the hydrogels synthesized using 1% of NMBAM. Diffusion behavior analyses determined that water diffusion into hydrogels followed the anomalous Fickian behavior. The as synthesized hydrogels were used in the removal of Remazol Red 3BS (RR3BS) dye from aqueous solutions, finding that the maximum dye adsorption capacity for an equilibrium aqueous concentration of 130 mg/L of RR3BS was 44.19 mg of RR3BS/g of dried hydrogel with 1% of NMBAM, with an adsorption mechanism well represented by the Langmuir model.

**Keywords** Hydrogel · Acrylamide · Acrylic acid · Remazol red dye · Water diffusion

**Electronic supplementary material** The online version of this article (doi:10.1007/s00396-016-3996-2) contains supplementary material, which is available to authorized users.

✉ Miguel A. Corona-Rivera  
coronamiguelangel@yahoo.com.mx

✉ Víctor M. Ovando-Medina  
ovandomedina@yahoo.com.mx

<sup>1</sup> Ingeniería Química, Coordinación Académica Región Altiplano (COARA), Universidad Autónoma de San Luis Potosí, Carretera a Cedral KM 5+600, San José de las Trojes, 78700 Matehuala, SLP, Mexico

<sup>2</sup> CIEP, Facultad de Ingeniería, Universidad Autónoma de San Luis Potosí, Manuel Nava #8, Zona Universitaria, 78000 San Luis Potosí, Mexico

<sup>3</sup> Facultad de Ciencias Químicas, Universidad Autónoma de Nuevo León, Av. Universidad, Cd. Universitaria, 66451 San Nicolás de Los Garza, NL, Mexico

## Introduction

In the last decade, the increase in development of new materials with high water sorption such as hydrogels has become of higher interest due to their ecological applications in up taking of heavy metal, toxic organic compounds, and dyes from wastewater streams. Also, these materials are studied due to their promising applications, such as sensors, separation membranes, adsorbents, and materials with applications in medicine and pharmacy as drug delivery systems. Hydrogels are a group of homopolymers or copolymers with three-dimensional cross-linked networks [1–7] which are able to swell in the aqueous media; actually, they are also classified within the expandable polymeric networks. The nature of monomers that form hydrogels and cross-linking degree of polymer chains determine the mechanical and swelling properties of dried hydrogel and their applications. The most employed method to synthesize hydrogels is the classic free radical polymerization of water-soluble monomers, which include acrylic acid, acrylamide, and their derivatives by means

of polymerization processes like emulsion, microemulsion, or the sol-gel processes [8–10].

Colored dye wastewater arises as a direct result of the production of the dye and also as a consequence of its use in the textile and other industries. There are more than 100,000 commercially available dyes with over  $7 \times 10^5$  t of dyes annually produced. It is estimated that 2% of dyes annually produced are discharged in effluents related with manufacturing processes, whereas 10% of dyes annually produced are discharged in effluents associated with textile industries [11–13]. Even if wastewaters contain low concentration of dye, they present strong color and turbidity, and their discharge is particularly difficult because of its negative visual impact. Discoloration of effluents is a well-known technical problem and therefore the researches are focused in finding effective treatments and materials capable of solving this problem [14–17]. For example, some researchers have used hydrogels in order to remove acidic and basic dyes from aqueous solutions [18, 19]. Karadag et al. [20] synthesized acrylamide (AAM)/maleic acid (MA) hydrogels by free radical polymerization in aqueous solution with some multifunctional cross-linking agent such as trimethylolpropane triacrylate and 1,4-butanediol dimethacrylate. These researchers used the synthesized hydrogels in experiments of swelling and adsorption of a water-soluble monovalent cationic dye such as Basic Blue 17 (Toluidin Blue). They observed swelling percentage between 1660 and 6050% in water (approximately 16.6 to 60.5 g of water/g of dried hydrogel), while dye adsorption increased according to the content of MA in the hydrogels. Duran et al. [19] reported the synthesis of acrylamide (AAM)–acrylic acid (AAc) hydrogels at AAM initial compositions of 15, 20, and 30%. The AAM–AAc monomer mixtures were irradiated under a  $^{60}\text{Co}$ - $\gamma$  source at different doses. The hydrogels were swollen in distilled water at different pH. The results of their swelling test at pH 8.0 indicated that poly(AAM–AAc) hydrogels at 15% of AAM have a maximum swelling of 3000% (30 g of water/g of dried hydrogel). The synthesized hydrogels were used in the removal of some textile dyes from aqueous solutions such as Janus Green B dye (JGB) in which the hydrogels showed the highest adsorption capacity (35 mg of dye/g of dried hydrogel at an equilibrium aqueous concentration of 4.8 mg/L), while the Congo Red dye (CR) was not adsorbed by hydrogels. Rojas et al. [21] reported

the polymerization of acrylamide in presence of poly(acrylic acid) using ammonium persulphate (APS) as initiator, NMBAM as cross-linking agent, and varying the AAM/poly(-acrylic acid) ratio, obtaining interpenetrated networks (IPN). Additionally, poly(acrylamide-co-acrylic acid) hydrogels were synthesized and characterized to compare with the IPNs. Absorption studies of pure water and metallic salt aqueous solutions were carried out observing a larger swelling degree when the concentration of PAAc was increased and the percentage of NMBAM decreased. The synthesized hydrogels in a 60/40 weight ratio of AAM/PAAc showed the best absorption properties of water and  $\text{Mg}^{2+}$  and  $\text{Cu}^{2+}$  ions in aqueous solutions.

Taking into account some reports about poly(AAM-co-AAc) hydrogels as background, and because to the best of our knowledge none hydrogel (synthetic or natural) has been applied to the removal of RR3BS dye (Fig. 1) from aqueous solutions, in this work, the effects of AAM/AAc ratio and the cross-linking agent concentration on the swelling performance were studied. Also, three different mathematical models were used to describe the swelling kinetic, water diffusion mechanism, and water absorption rate. The as synthesized hydrogels were used in the removal of RR3BS dye from aqueous solutions. We also tried to elucidate the adsorption mechanism of the dye onto hydrogels.

## Experimental

### Materials

AAM, AAc, V-50, and NMBAM with purity of 99% were purchased from Sigma-Aldrich and used as received. RR3BS dye (C.I. 239) was kindly donated by a textile industry of San Luis Potosí, Mexico. Bidistilled water was used in all the experiments.

### Hydrogel synthesis

Cross-linked copolymers of acrylic acid and acrylamide were synthesized by radical polymerization in aqueous solutions. Table 1 summarizes the compositions of the monomer mixtures (in grams) and the amount of the copolymer used in each

**Fig. 1** Chemical structure of Remazol Red dye (RR3BS)

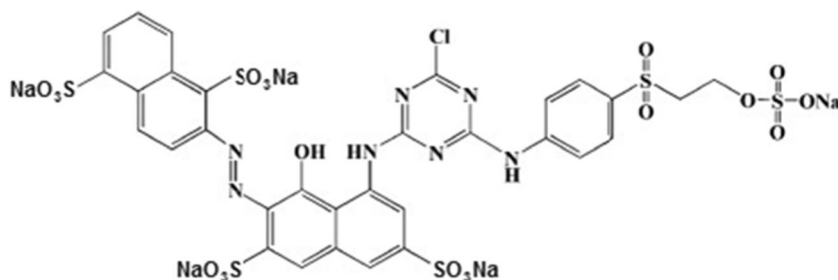


**Table 1** Compositions used in the synthesis of hydrogels

Run	AAM (g)	AAc (g)	NMBAM (g)
1-AAM/AAc 100/0	3.0	0	0.03
2-AAM/AAc 90/10	2.7	0.3	0.03
3-AAM/AAc 80/20	2.4	0.6	0.03
4-AAM/AAc 70/30	2.1	0.9	0.03
5-AAM/AAc 60/40	1.8	1.2	0.03
6-AAM/AAc 100/0	3.0	0	0.06
7-AAM/AAc 90/10	2.7	0.3	0.06
8-AAM/AAc 80/20	2.4	0.6	0.06
9-AAM/AAc 70/30	2.1	0.9	0.06
10-AAM/AAc 60/40	1.8	1.2	0.06

run. For all samples, the polymerization process was made as follows: a mixture of water (27 g) and AAM was poured in a cylindrical glass vial of 40 mL with mild stirring until dissolution. Then, AAc was added to this previous mixture and homogenized. After this, NMBAM was added and the resulted mixture was immersed into a water bath with constant temperature under mild magnetic stirring (avoiding burble formation). In order to start the polymerization, the initiator V-50 (0.03 g) was added to the reaction mixture and the process was stopped after 2 h of polymerization.

After this period, the glass vials were broken for extracting the samples and keeping the cylindrical geometry of the hydrogels. All the hydrogel samples were cut into small disks of 2 cm diameter and 0.5 cm height. These sample disks were immersed in 1.0 L of distilled water for a period of 24 h to remove the unreacted components and dried at 40 °C until constant weight (5 days approximately). The dried hydrogels were analyzed by Raman spectroscopy using a high resolution Raman spectrometer (Horiba Jobin-Yvon, LabRAM HR 800). Zero point charge (ZPC) of hydrogels was determined as follows: 50 mL of distilled water was poured into a 100-mL Erlenmeyer flask, adjusting the initial pH between 2 and 11 by adding HCl or NaOH 0.1 N solutions. Afterwards, 0.5 g of dried hydrogel was added, and after 48 h of magnetic stirring at room temperature, the final pH was measured. The ZPC corresponds to the point where the curve of final pH as a function of initial pH crosses the diagonal at 45°.

### Hydrogel swelling experiments

The swelling performance of hydrogels was determined immersing the dried hydrogel disks (previously weighed) in distilled water at room temperature (25 °C). The hydrogel swelling was calculated following the changes in the weight at different intervals of time. This monitoring

was carried out until almost no variation in the weight of the hydrogels was observed. The swelling percentage per gram of dried hydrogel ( $S$ ) and the water absorbed percentage ( $W$ ) were calculated with the following equations:

$$S = \frac{m_t - m_0}{m_0} \times 100\% \quad (1)$$

$$W = \frac{m_t - m_0}{m_t} \times 100\% \quad (2)$$

where  $m_t$  is the mass of swollen hydrogel at a given time and  $m_0$  represents the mass of dried hydrogel.

### Remazol red dye adsorption

Adsorption experiments were made using batch reactors at 25 °C and pH value of 3 as follows: 0.2 g of dried hydrogel was added to a conical vial of 50 mL and then, 40 mL of RR3BS in a range concentration of 30 to 300 mg/L (sorbent dose of 0.2 g was chosen because it was observed from preliminary experiments that this value does not affect dye concentration due to hydrogel swelling). Vials were maintained under stirring into an orbital shaker (INO 650V-7) at constant temperature. The solution pHs were adjusted using a pH meter (Thermo Scientific, Orion 3 Star) with the addition of HCl or NaOH 0.1 N during 10 days (time required to reach the equilibrium adsorption). The adsorbed dye mass was calculated by a mass balance between the initial ( $C_0$ ) and final concentrations ( $C_{eq}$ ) of the solutions.  $C_0$  and  $C_{eq}$  were determined in a spectrophotometer (Genesis 10S UV/Vis) using a calibration curve with standard solutions in the concentration range of 5 to 20 mg/L at  $\lambda = 600$  nm.

### Water absorbency mathematical models

#### Swelling kinetic

The controlling mechanism of hydrogel swelling was analyzed using a simple second-order model in the following form [22]:

$$\frac{dq}{dt} = k_{2,S} (q_{eq} - q)^2 \quad (3)$$

where  $q$  represents the weight swelling ratio and is given by  $m_t/m_0$  as defined in Eq. (1),  $t$  is the time in hours,  $k_{2,S}$  is the rate constant of swelling, and  $q_{eq}$  denotes the weight swelling ratio at equilibrium. The integration of Eq. (3) gives the following:

$$k_{2,S}t = \frac{1}{(q_{eq} - q)} - \frac{1}{q_{eq}} \quad (4)$$

Equation (4) can be rearranged as follows:

$$\frac{t}{q} = \frac{1}{k_{2,s}q_{\text{eq}}^2} + \frac{1}{q_{\text{eq}}}t \quad (5)$$

In Eq. (5),  $1/k_{2,s}q_{\text{eq}}^2$  is the reciprocal of the initial swelling rate of hydrogel,  $r_0$ ; the value of  $1/q_{\text{eq}}$  represents the reciprocal of equilibrium swelling ratio (the maximum theoretical),  $q_{\text{max}}$ . These values were determined from a plot of the experimental values of  $t/q$  against  $t$ .

### Water diffusion mechanism

Water diffusion mechanism into hydrogels during the swelling was analyzed using the well-known power-law model [23–25]:

$$F_{\text{sp}} = \frac{m_t - m_0}{m_0} = Kt^n \quad (6)$$

where  $K$  is the swelling constant which takes into account the characteristic of macromolecular network system and the penetrant (water), whereas  $n$  is the swelling (diffusional) exponent, which is indicative of the transport mechanism. Equation (6) describing both Fickian and non-Fickian transport behavior of water into a polymeric matrix is valid for the first 60% of the fractional water uptake.

### Water sorption rate

Water sorption rate constant,  $K_{\text{sr}}$ , is an important diffusional parameter, which can be related to hydrophilic character of polymeric network and can be calculated using the following equation [4, 26]:

$$-\ln\left(1 - \frac{m_t}{m_s}\right) = K_{\text{sr}}t + E \quad (7)$$

where  $m_t$  is the sorption water amount at time  $t$ ,  $m_s$  is the water sorption amount at equilibrium, and  $E$  is a constant.  $K_{\text{sr}}$  was calculated from the slope of linear plot of  $-\ln(1 - m_t/m_s)$  vs.  $t$ .

## Results and discussion

### Hydrogel composition

The chemical composition of hydrogel chains is very important because it determines their applicability. For example, the carboxylic groups due to a monomer like AAc can affect the hydrogel performance in ionic interchange processes. Also, the hydrogel swelling ability and dye adsorption will depend on the copolymer composition moieties and the cross-linking degree. Figure 2 shows a proposed chemical structure of the copolymer of acrylamide with acrylic acid cross-linked with

NMBAM. Although the monomers are water soluble, the resulting hydrogel is not. It can be seen from Fig. 2 that NMBAM allows the formation of three-dimensional structures reacting through its two functional groups. Furthermore, the pendant carboxylic groups of AAc are available to act as ion interchangers.

Figure 3 shows Raman spectra of hydrogels obtained at different AAm/AAc weight ratios (100/0, 90/10, 80/20, 70/30, and 60/40) with 1% of NMBAM (runs 1 to 5 in Table 1). From this figure, it can be appreciated a peak around  $1714 \text{ cm}^{-1}$  (marked with arrows) for runs 3-AAm/AAc 80/20, 4-AAm/AAc 70/30, and 5-AAm/AAc 60/40. In contrast, this signal is not observed for run 1-AAm/AAc 100/0 and 2-AAm/AAc 90/10 corresponding to AAm/AAc ratio of 100/0 and 90/10, respectively. In the first case, it was expected since the sample of 1-AAm/AAc 100/0 is basically a homopolymer of AAm and this peak is ascribed to carboxylic groups of the AAc units in the hydrogels. In run AAm/AAc ratio of 90/10, this signal is also not perceptible due to the low amount of AAc used. Similar results were observed for hydrogels synthesized with 2% of cross-linking agent.

Table 2 resumes the different vibrational assignments of Raman spectra, which agree with the reported in the literature for the homopolymer of acrylamide [27] and with the Raman spectrum of acrylic acid [28]. The signals corresponding to NMBAM overlap with the AAm peaks.

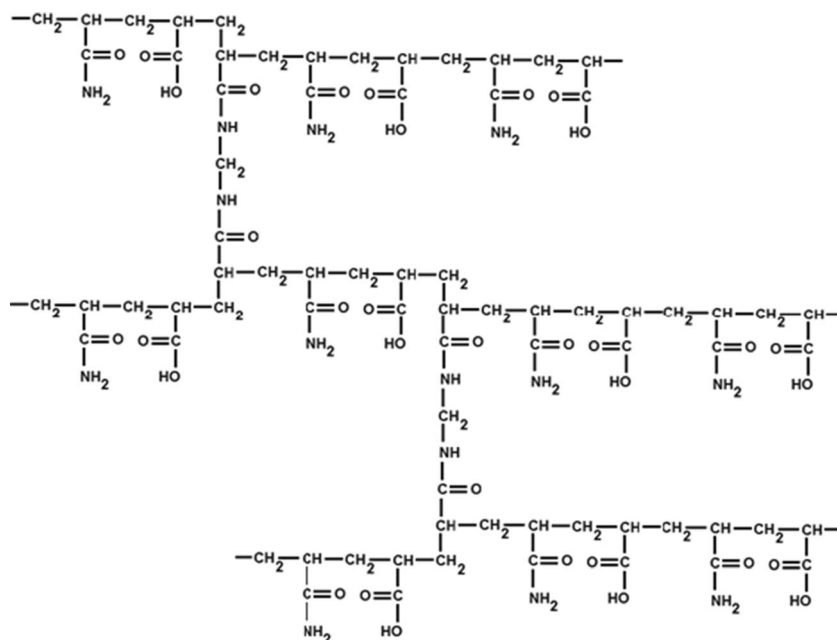
### Hydrogel swelling percentage

Figures 4 and 5 show the results of  $S$  (a) and  $W$  (b) for different AAm/AAc ratios and contents of 1 and 2% of cross-linking agent, respectively. Cross-linking chains directly affect the length of the polymeric chain segment and the pore size of the cross-linked network. Because hydrogels were swollen at different rates, the time was normalized (relative time) in Figs. 4a and 5a. The relative time was calculated dividing the time by the total time required to reach the maximum swelling.

It can be seen from Figs. 4a and 5a that the water sorption capacity of the hydrogels increases with the content of the acrylic acid in the hydrogel and decreases with the cross-linking agent percentage. The maximum swelling was observed for AAm/AAc ratio of 70/30 ( $S = 7000$  and  $2700\%$  for 1 and 2% of NMBAM, respectively). Clearly, the acrylic acid has a strong influence on the water sorption capacity of hydrogels. However, when the hydrogel has the maximum amount tested of AAc (AAm/AAc = 60/40), the swelling property decreases. The presence of acrylic acid in the hydrogel enhances the hydrophilicity, but on the other hand, the excess of AAc affects the three-dimensional stability of hydrogels, conferring poor mechanical properties [34].

Moreover, swelling capacity of the hydrogel was also affected when the amount of cross-linking agent was increased

**Fig. 2** Proposed chemical structure of the copolymer of acrylamide/acrylic acid cross-linked with NMBAM



(2%); it can be explained as narrower pores are formed in the hydrogel with 2% of NMBAM in comparison with the hydrogel of 1% (Fig. 3S and 4S of supplementary information). In other words, less space for incorporating water molecules can be expected in the hydrogel with higher amount of cross-linking which results in a more rigid polymer due to an increase of bridging between chains. It can be perceived in Figs. 4b and 5b that more than 80% of water sorption was reached after approximately 5 h, and sorption equilibrium was reached after 20 and 30 h for hydrogels with 1 and 2% of NMBAM (insets), respectively.

### Swelling kinetic

The swelling kinetic rates of hydrogels were examined with Eq. (5) to determine the controlling mechanism of the swelling process. The great number and array of different chemical

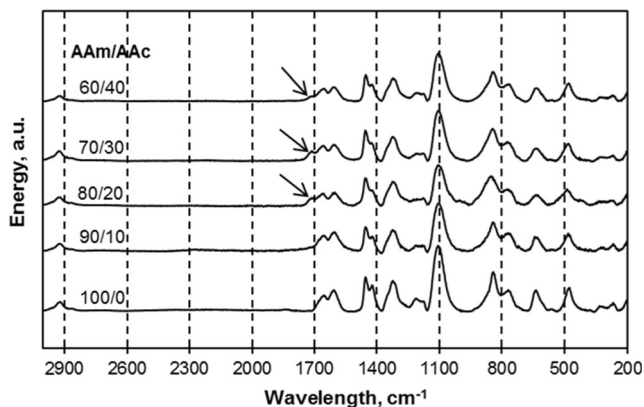
groups on the poly(AAm-co-AAc) chains (such as amine, carbonyl, and carboxyl) imply that there are many types of polymer–water interactions. Figure 6 shows the experimental and fitted values of  $t/q$  as a function of  $t$  for hydrogels synthesized with 2% of the cross-linking NMBAM. The calculated

**Table 2** Vibrational assignments of Raman spectra of polyacrylamide-co-polyacrylic acid cross-linked with NMBAM

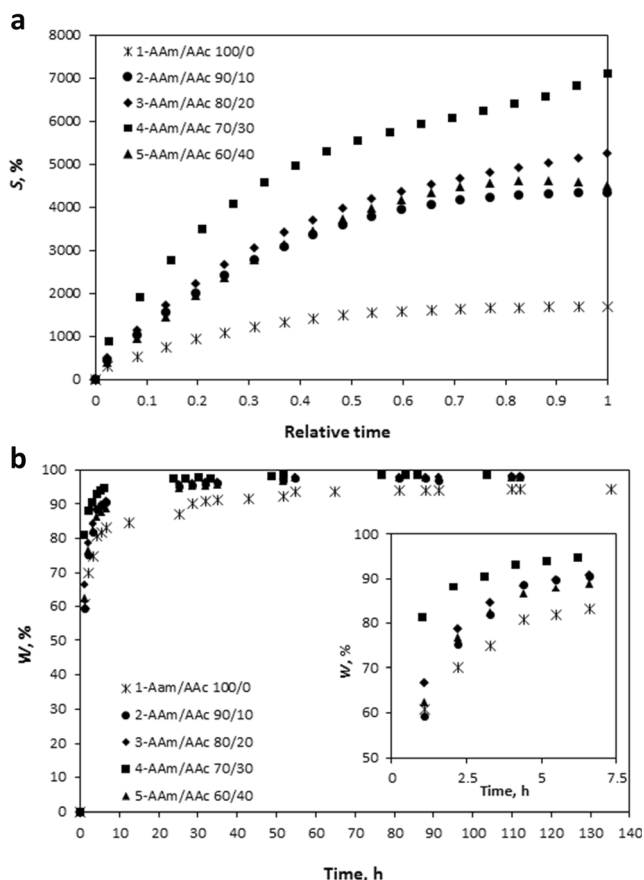
Obtained frequency	Type of vibration <sup>a</sup>
2926-W	CH <sub>2</sub> -ν <sub>s</sub>
2867-W	CH-ν
1714-M	COO-ν <sub>a</sub>
1655-M	CON-ν
1608-MS	NH <sub>2</sub> -δ
1454-M	CH <sub>2</sub> -δ
1423-M	C-N-ν
1323-M	CH <sub>2</sub> -ω
1216-W	NH <sub>2</sub> -ω
1174-W	CC-ν <sub>a</sub>
1107-S	C-C-ν <sub>a</sub>
844-W	CH <sub>2</sub> -Γ
768-W	C-H-ω
639-M	C-O-ω
480-S	C-C-δ <sub>b</sub>
327-W	C-C-δ <sub>a</sub>
261-W	C-C-δ <sub>b</sub>

M medium, W weak, VW very weak, VVW very very weak, MS medium strong, VS very strong, ν<sub>a</sub> asym. stretching, ν<sub>s</sub> sym. stretching, δ deformation, ω wagging, Γ twisting, δ<sub>b</sub> and δ<sub>a</sub> = asymmetric bending, τ torsion

<sup>a</sup> S strong



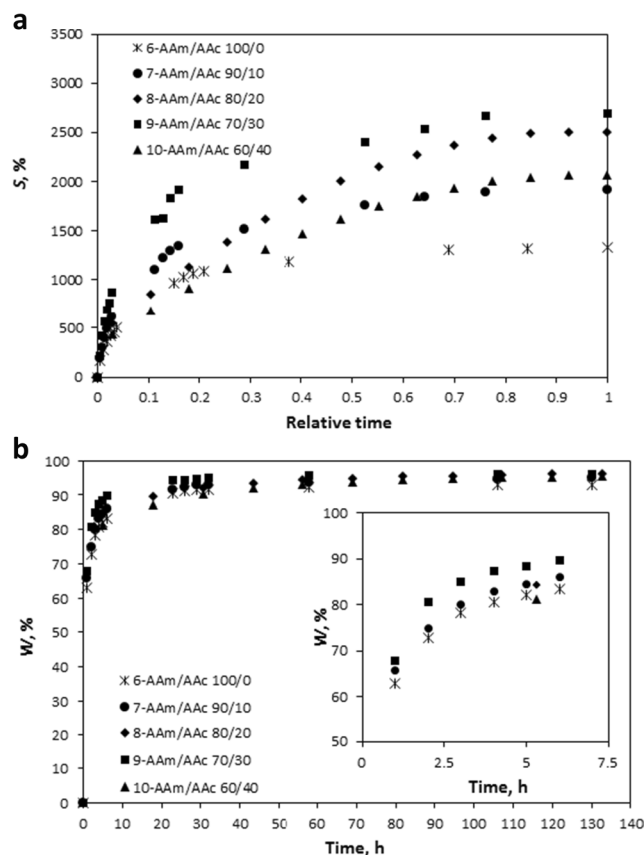
**Fig. 3** Raman spectra of hydrogels obtained at different AAm/AAc ratios with 1% of NMBAM



**Fig. 4** Hydrogel water sorption as a function of AAm/AAc ratio for 1% of cross-linking agent. **a** Swelling percentage. **b** Water absorbed percentage

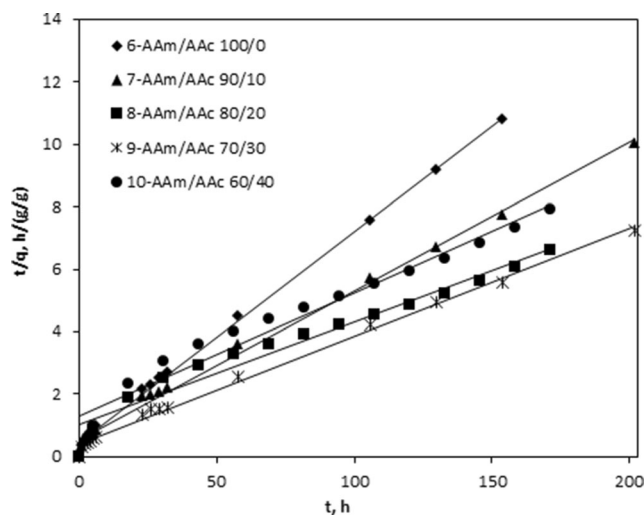
values of  $R^2$  of fitting were greater than 0.97, demonstrating relatively good agreement with the second-order mathematical model.

Table 3 shows the calculated swelling kinetic parameters of second-order mathematical model. It can be seen that  $r_0$  value is increased with the AAc content and decreases with the cross-linking agent amount, except for hydrogel with 100/0 of AAm/AAc ratio, which showed a value two times higher than hydrogels with 10 and 20% of AAc; however, hydrogel with 70/30 of AAm/AAc ratio showed the optimized composition in respect to initial swelling rate. At high amounts of AAc in the hydrogel,  $r_0$  values start to decrease due to poor mechanical properties of hydrogel (swelled hydrogel shatters). On the other hand,  $k_{2s}$  values can be related to ionization changes of functional groups of hydrogels [25, 26, 29], that is, by increasing the NMBAM percentage, more NH groups are present in the hydrogel chains, resulting in greater  $k_{2s}$  values, nevertheless independently of hydrogel cross-linking degree  $k_{2s}$  decreases with the AAc content. In other words,  $\text{NH}_2$  and NH groups just affect the swelling rate, but not the maximum swelling capacity,  $q_{\max}$ , which increased with AAc content and decreased with the NMBAM amount. This behavior is expected since



**Fig. 5** Hydrogel water sorption as a function of AAm/AAc ratio for 2% of cross-linking agent. **a** Swelling percentage. **b** Water absorbed percentage

hydrophilicity of hydrogel net is enhanced with density of carboxylic groups of AAc in structure. However, the increase in the NMBAM percentage makes the structure constricted for water to diffuse. These two factors determine the rate of hydrogel swelling.



**Fig. 6** Swelling rate plot of hydrogels at 2% of NMBAM

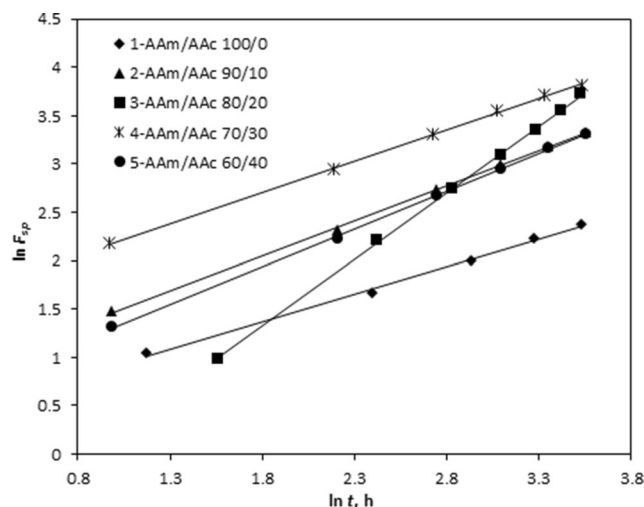
**Table 3** Swelling rate parameters of hydrogel of poly(AAm-co-AAc)

AAm/AAc	NMBAM	
	1%	2%
Initial swelling rate, $r_0$		
100/0	1.062	2.180
90/10	2.000	1.892
80/20	2.023	0.962
70/30	3.632	2.239
60/40	1.458	0.604
Swelling rate constant, $k_{2s} \times 10^3$		
100/0	3.373	10.844
90/10	1.029	4.778
80/20	0.743	1.419
70/30	0.760	2.927
60/40	0.661	1.296
Maximum (theoretical) weight swelling ratio, $q_{max}$		
100/0	20.408	14.858
90/10	55.866	21.001
80/20	67.114	30.487
70/30	82.644	29.325
60/40	69.930	27.472

### Water diffusion mechanism

Swelling properties and diffusional behavior of hydrogels are the key for their use in environmental, biomedical, pharmaceutical, and industrial applications as agricultural. For example, knowledge about swelling kinetics is important for designing controlled-release systems for drugs and agriculture pesticides based on swellable polymer matrices and for predicting the release rates of the active ingredients as fertilizers. When a dried hydrogel becomes in contact with water, water molecules diffuse into hydrogel, resulting in the relaxation of its macromolecular chains [28]. Water diffusion can be into pre-existing or dynamically formed spaces between hydrogel chains, involving larger segmental motion resulting in an increased separation between hydrogel chains.

Figure 7 shows a plot of experimental values of  $\ln F_{sp}$  as a function of  $\ln t$  for synthesized hydrogels with 1% of NMBAM and the calculated values of  $\ln F_{sp}$  using the model described in Eq. (6). A good agreement can be seen between experimental data and mathematical model. Swelling exponents of Eq. (6),  $n$ , and swelling constants,  $K$  for each hydrogel, were calculated from the slopes and intercepts of the lines, respectively, and are listed in Table 4. Table 4 shows that the number determining the type of diffusion  $n$  is over 0.50 with exception of hydrogels with 80/20 and 60/40 of AAm/AAc ratio (2% of NMBAM). According to the relative rates of diffusion ( $R_d$ ) and polymer relaxation ( $R_r$ ), three classes of diffusion can be distinguished. For a planar geometry, the

**Fig. 7**  $\ln F_{sp}$  as a function of  $\ln t$  of poly(AAm-co-AAc) hydrogels with 1% of NMBAM

value of (a)  $n = 0.5$  indicates a Fickian diffusion mechanism (case I) in which the rate of diffusion is much smaller than the rate of relaxation ( $R_d \ll R_r$ , system controlled by diffusion), (b)  $n = 1.0$  indicates case II, where the diffusion process is much faster than the relaxation process ( $R_d \gg R_r$ , system controlled by relaxation), and (c)  $0.5 < n < 1.0$  indicates non-Fickian (anomalous) diffusion mechanism, which describes those cases where the diffusion and relaxation rates are comparable ( $R_d \sim R_r$ ) [30]. Therefore, in our case, with the exception of hydrogels with 80/20 and 60/40 of AAm/AAc ratio (2% of NMBAM), the diffusion of water into the hydrogels corresponds to an anomalous behavior; this implies that relaxation and diffusion time are of the same order of magnitude. As water diffuses into the hydrogel, rearrangement of chains does not occur immediately [23, 26].

**Table 4** Swelling exponent and swelling constant of hydrogel of poly(AAm-co-AAc)

AAm/AAc, wt/wt	NMBAM	
	1%	2%
Swelling exponent, $n$		
100/0	0.56	0.55
90/10	0.72	0.55
80/20	0.73	0.50
70/30	0.65	0.63
60/40	0.79	0.50
Swelling constant, $K, h^{-n}$		
100/0	0.35	0.61
90/10	0.75	0.75
80/20	0.84	0.87
70/30	1.55	0.95
60/40	0.52	0.64

## Water sorption rate

Table 5 shows the water sorption rate constant of hydrogels with different AAm/AAC ratios for 1 and 2% of cross-linking NMBAM. It can be observed that for 1% of NMBAM, the AAC content does not have an important effect on  $K_{sr}$ , ranging from  $35.2 \times 10^{-3}$  to  $49.6 \times 10^{-3}$ ; on the other hand, when NMBAM was increased to 2%,  $K_{sr}$  for hydrogel with AAm/AAC ratio of 100/0 increased compared to that observed for 1%; however,  $K_{sr}$  values decreased noticeably when AAC is present, even for low AAC concentrations. This behavior may be ascribed to hydrophilic characteristics of AAC. AAC units can interact with water molecules, and sorption may be slower, which was more noticeable for hydrogels with 2% of cross-linking agent.

## Dye adsorption experiments

Different adsorbents present divergent ranges of suitable pH solution, depending on dye nature. The reason that a pH 3 was chosen is because from zero point charge (ZPC) of used hydrogel was 2.9 (Fig. S1 in supplementary information), and the dye dissociates with negative charges (Fig. 1). If ZPC was 2.9, then adsorbent's surface was positively charged at solution pH below 2.9, causing better RR3BS anion adsorption through the electrostatic attraction phenomenon. On the other hand, above the ZPC, surface of adsorbent was negatively charged; this causes competition between RR3BS formed anions for adsorption locations as well as the repulsion of anionic RR3BS molecules, resulting in the reduction of dye removal efficiency. Samples of hydrogels corresponding to runs 4-AAm/AAC 70/30 and 9-AAm/AAC 70/30 were selected to make the dye adsorption experiments because they showed the best swelling capacity. It is well known that adsorption process of a solute onto an adsorbent can be described by many adsorption isotherm models. The equilibrium adsorption isotherms are of fundamental importance in the design of any adsorption system. In this work, the experimental data of adsorption capacity in aqueous solutions were adjusted by Langmuir and Freundlich mathematical models, observing better adjustment with the Langmuir equation:

$$q = q_m K_L C_e / (1 + K_L C_e) \quad (8)$$

where  $q$  is the adsorption capacity at the equilibrium concentration  $C_e$ ,  $K_L$  is a Langmuir constant parameter, and  $q_m$  is the maximum adsorption capacity. The constants for these isotherms were evaluated by the least-squares method based on an optimization algorithm. The obtained Langmuir parameters are presented in Table 6.

Figure 8a, b shows correlation between experimental data and Langmuir isotherms of RR3BS dye onto the hydrogel 4-AAm/AAC 70/30 and 9-AAm/AAC 70/30 for 1 and 2% of

**Table 5** Sorption rate constant ( $K_{sr} \times 10^3$ ) of hydrogel of poly(AAm-co-AAc)

AAm/AAC	NMBAM	
	1%	2%
100/0	44.6	52.7
90/10	47.9	27.2
80/20	35.2	27.0
70/30	49.6	28.2
60/40	45.2	23.6

NMBAM, respectively; which indicates an increase of 19% of adsorption capacity of RR3BS comparing the values of  $q_m$ . Since the amount of AAm is higher in the hydrogel (70%), it can be expected that the adsorption process is regulated by the amide groups which can interact with the dye ions by ion exchange. This is also related with the swelling capacity associated by the porous size (cross-linking level) and the hydrophilicity (AAC amount).

Adsorption capacities of hydrogels reported in the present study are comparable to some other polymeric materials regarding to RR3BS dye removal from aqueous solutions. For example, Kyzas et al. [31] reported that materials composed of polymeric molecular imprinted  $\beta$ -cyclodextrin and chitosan at 25 °C showed a maximum amount of adsorbed ( $q_m$  calculated from their experimental data) RR3BS dye of 35 mg/g for a final equilibrium dye concentration of 32 mg/L. Both hydrogels (AAm/AAC 70/30 with 1 and 2%) synthesized in the present work showed more adsorption capacity (Table 6) than those materials and with the advantage that molecular imprinted process is also more complex and expensive. On the other hand, cheap and available materials such as activated carbon obtained from sawdust have also been tested in the RR3BS dye removal, as reported by Ara et al. [32] at 25 °C, who tested dye concentrations in the range of 50 to 200 mg/L, observing that maximum uptake level reached was almost ten times smaller ( $q_m = 2.36$  mg/g according to Langmuir isotherm) than our AAm/AAC (70/30) hydrogel with 1% of NMBAM. Furthermore, Hafez et al. [33] used polyvinylpyrrolidone/AAC hydrogels mixed with TiO<sub>2</sub> particles in the adsorption of RR3BS dye (unreported temperature and initial dye concentration of 56 mg/L) followed by photodegradation, observing a  $q_m$  of 6.6 mg/g. In summary,

**Table 6** Langmuir model parameters

Run	$q_m$	$K_L$	$R^2$
4-AAm/AAC 70/30	44.19	$6.93 \times 10^{-3}$	0.9901
9-AAm/AAC 70/30	38.17	$7.67 \times 10^{-3}$	0.9923

$q_m$  in mg/g,  $K_L$  in L/mg, and  $R$  represents the correlation factor of regression



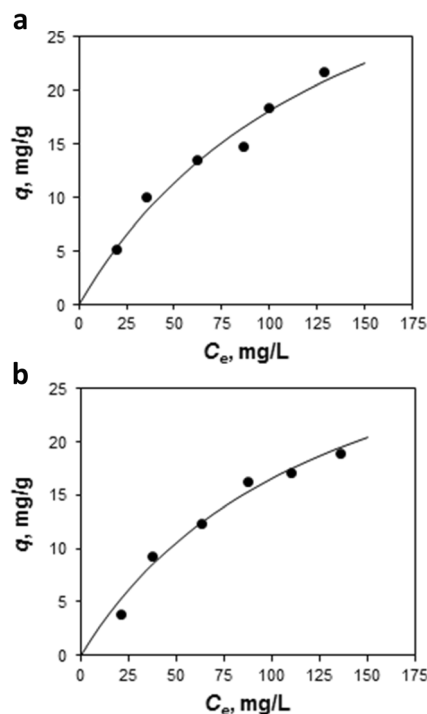


**Fig. 8** Adsorption isotherms for RR3BS dye on hydrogels obtained with AAm/AAC ratio of 70/30 and different amounts of NMBAM. **a** 1% NMBAM. **b** 2% NMBAM, at 25 °C. The *filled circles* represent experimental data and the *continuous curves* are data calculated with the Langmuir model

the adsorption results showed in the present work concerning AAm/AAC hydrogels suggest their potential application in the treatment of textile wastewaters where Remazol Red dye and similar dyes are present.

Hydrogels were tested for reusability by adsorption–desorption experiments, which are shown in supplementary information (Fig. S2). It was observed from these experiments that for high initial dye concentration, some of dye remains adsorbed onto hydrogel after desorption (100 and 150 mg/L), which can be due to strong interaction between hydrogel surface and molecules of dye, which cannot be desorbed by the process used for desorption. However, the reusability was demonstrated for low initial dye concentration (50 mg/L).

## Conclusions

Cross-linked hydrogels of poly(AAm-co-AAC) were synthesized by free radical copolymerization with NMBAM as cross-linker. It was observed that water sorption capacity of the hydrogels increases with the content of acrylic acid and decreases with the cross-linking agent percentage. However, when the amount of AAC was higher than 30%, the swelling decreased, which was ascribed to poor mechanical properties. The best swelling was observed for hydrogel with AAm/AAC 70/30 weight ratio cross-linked with 1% of NMBAM,

observing approximately 7000% of swelling. Water absorbency analysis demonstrated that swelling kinetic can be well represented by a second-order kinetic model, and that diffusion of water into the hydrogels corresponds to anomalous behavior, which implies hydrogel chain relaxation and water diffusion time are of the same magnitude order. These hydrogels were used in the removal of RR3BS dye from aqueous solutions, finding that the adsorption process was well represented by the Langmuir model, with a maximum adsorption capacity of 44.2 and 38.2 mg/g for 1 and 2% of NMBAM, respectively, at the equilibrium. This adsorption capacity is comparable or even better with some other materials, already reported, used for the same application purpose.

**Acknowledgements** This work was supported by the Consejo Nacional de Ciencia y Tecnología (México) for grant no. CB-169444. Author I.D. Antonio-Carmona acknowledges the financial support to PRODEP-SEP for postdoctoral position with the Academic Group of Ingeniería de Procesos Químicos y Ambientales (UASLP-CA-202).

## Compliance with ethical standards

**Conflict of interest** The authors declare that they have no conflict of interest.

## References

- Xue W, Champ S, Huglin MB (2001) Network and swelling parameters of chemically crosslinked thermoreversible hydrogels. *Polymer* 42:3665–3669. doi:10.1016/S0032-3861(00)00627-3
- Nguyen KT, West JL (2002) Photopolymerizable hydrogels for tissue engineering applications. *Biomaterial* 23:4307–4314. doi:10.1016/S0142-9612(02)00175-8
- Liu MZ, Liang R, Zhan FL, Liu Z, Niu AZ (2006) Synthesis of a slow-release and superabsorbent nitrogen fertilizer and its properties. *Polym Adv Technol* 47:430–438. doi:10.1002/pat.720
- Ali AE, Shawky HA, Abd El Rehim HA, Hegazy EA (2003) Synthesis and characterization of PVP/AAC copolymer hydrogel and its applications in the removal of heavy metals from aqueous solution. *Eur Polym J* 39:2337–2344. doi:10.1016/S0014-3057(03)00150-2
- Peppas NA, Bures P, Leobandung W, Ichikawa H (2000) Hydrogels in pharmaceutical formulations. *Eur J Pharm Biopharm* 50:27–46. doi:10.1016/S0939-6411(00)00090-4
- Kopecek J (2007) Hydrogel biomaterials: a smart future? *Biomaterials* 28:5185–5192. doi:10.1016/j.biomaterials.2007.07.044
- Lutolf MP (2009) Biomaterials: spotlight on hydrogels. *Nat Mater* 8:451–453. doi:10.1038/nmat2458
- Maitra J, Shukla VK (2014) Cross-linking in hydrogels—a review. *AM J Polym Sci* 4:25–31. doi:10.5923/j.ajps.20140402.01
- Alemzadeh I, Vossoughi M (2002) Controlled release of paraquat from poly vinyl alcohol hydrogel. *Chem Eng Process* 41:707–710. doi:10.1016/S0255-2701(01)00190-8
- Minhas M, Ahmad M, Ali L, Sohail M (2013) Synthesis of chemically cross-linked polyvinyl alcohol-co-poly (methacrylic acid) hydrogels by copolymerization; a potential graft-

- polymeric carrier for oral delivery of 5-fluorouracil. *J Pharm Sci* 21:1–9. doi:10.1186/2008-2231-21-44
11. Allen SJ, Koumanova B (2005) Decolourisation of water/wastewater using adsorption (review). *J U Chem Tech Metal* 40:175–192
  12. Khare SK, Panday KK, Srivastava RM, Singh VN (1987) Removal of victoria blue from aqueous solution by fly ash. *J Chem Tech Biotechnol* 38:99–104. doi:10.1002/jctb.280380206
  13. Karadag E, Saraydin D, Güven O (1996) Interaction of some cationic dyes with acrylamide/itaconic acid hydrogels. *J Appl Polym Sci* 61:2367–2372. doi:10.1002/(SICI)1097-4628(19960926)61:13<2367::AID-PP16>3.0.CO;2-1
  14. Rodriguez J, Rodrigo MA, Panizza M, Cerisola G (2009) Electrochemical oxidation of acid yellow 1 using diamond anode. *J Appl Electrochem* 39:2285–2289. doi:10.1007/s10800-009-9880-8
  15. Karadag E, Saraydin D, Güven O (1996) A study on the adsorption of some cationic dyes onto acrylamide/itaconic acid hydrogels. *Polym Bull* 36:745–752. doi:10.1007/BF00338639
  16. Saraydin D, Karadag E, Güven O (1996) Adsorption of some basic dyes by acrylamide-maleic acid hydrogels. *Separation Sci Technol* 31:423–434. doi:10.1080/01496399608000705
  17. Saraydin D, Karadag E, Güven O (1996) Behaviors of acrylamide/maleic acid hydrogels in uptake of some cationic dyes from aqueous solutions. *Separation Sci Technol* 31:2359–2371. doi:10.1080/01496399608001053
  18. Saraydin D, Karadag E, Güven O (2001) Use of superswelling acrylamide/maleic acid hydrogels for monovalent cationic dye adsorption. *Appl Polym Sci J* 79:1809–1815. doi:10.1002/1097-4628(20010307)79:10<1809::AID-PP90>3.0.CO;2-L
  19. Duran S, Solpan D, Güven O (1999) Synthesis and characterization of acrylamide-acrylic acid hydrogels and adsorption of some textile dyes. *Nucl Instr Meth B* 151:196–199. doi:10.1016/S0168-583X(99)00151-2
  20. Karadag E, Baris U, Saraydin D (2002) Swelling equilibria and dye adsorption studies of chemically crosslinked superabsorbent acrylamide/maleic acid hydrogels. *Eur Polym J* 38:2133–2141. doi:10.1016/S0014-3057(02)00117-9
  21. Rojas de Gásque B, Ramírez M, Prin JL, Torres C, Bejarano L, Villarroel H, Rojas L, Murillo M, Katime I (2010) Hidrogeles de acrilamida/ácido acrílico y de acrilamida/poli(ácido acrílico): estudio de su capacidad de remediación en efluentes industriales. *Rev Latinam Metal Mater* 30:28–39
  22. Peniche C, Cohen ME, Vazquez B, Roman JS (1997) Water sorption of flexible networks based on 2-hydroxyethyl methacrylate-triethylenglycol dimethacrylate copolymers. *Polymer* 38:5977–5982. doi:10.1016/S0032-3861(96)01058-0
  23. Peppas NA, Franson NM (1983) The swelling interface number as a criterion for prediction of diffusional solute release mechanisms in swellable polymers. *J Polym Sci Pol Phys* 21:983–997. doi:10.1002/pol.1983.180210614
  24. Ritger PL, Peppas NA (1987) A simple equation for description of solute release II. Fickian and anomalous release from swellable devices. *J Control Release* 5:37–42. doi:10.1016/0168-3659(87)90035-6
  25. Ostrowska-Czubenko J, Gierszewska M, Pieróg M (2015) pH-responsive hydrogel membranes based on modified chitosan: water transport and kinetics of swelling. *J Polym Res* 22:153–164. doi:10.1007/s10965-015-0786-3
  26. Karadag E, Saraydin D, Güven O (2004) Water absorbency studies of  $\gamma$ -radiation crosslinked poly (acrylamide-co-2, 3-dihydroxybutanedioic acid) hydrogels. *Nucl Instrum Methods Phys Res, Sect B* 225:489–496. doi:10.1016/j.nimb.2004.06.010
  27. Murugan R, Mohan S, Bigotto A (1998) FTIR and polarised Raman spectra of acrylamide and polyacrylamide. *J Korean Phys Soc* 32:505–512
  28. Chitra M, Yang S (2010) Pressure-induced polymerization of acrylic acid: a Raman spectroscopic study. *J Phys Chem B* 114:9744–9750. doi:10.1021/jp1034757
  29. Guilherme MR, Moia TA, Reis AV, Paulino AT, Rubira AF, Mattoso LHC, Muniz EC, Tambourgi EB (2009) Synthesis and water absorption transport mechanism of a pH-sensitive polymer network structured on vinyl-functionalized pectin. *Biomacromolecules* 10:190–196. doi:10.1021/bm801250p
  30. Gierszewska-Drużyńska M, Ostrowska-Czubenko J (2012) Mechanism of water diffusion into noncrosslinked and ionically crosslinked chitosan membranes. *Journal Progress on Chemistry and Application of Chitin and Its Derivates* 17:59–66
  31. Kyzas GZ, Lazaridis NK, Bikiaris DN (2013) Optimization of chitosan and  $\beta$ -cyclodextrin molecularly imprinted polymer synthesis for dye adsorption. *Carbohydr Polym* 91:198–208. doi:10.1016/j.carbpol.2012.08.016
  32. Ara NJ, Hasan MA, Rahman MA, Salam MA, Salam A, Shafiqul A (2013) Removal of remazol red from textile waste water using treated sawdust—an effective way of effluent treatment. *Bangl Pharm J* 16:93–98. doi:10.3329/bpj.v16i1.14501
  33. Hafez HS, El-Hag Ali A, Abdel-Mottaleb MSA (2005) Photocatalytic efficiency of titanium dioxide immobilized on PVP/AAC hydrogel membranes: a comparative study for safe disposal of wastewater of remazol red RB-133 textile dye. *Int J Photoenergy* 7:181–185. doi:10.1155/S1110662X05000279
  34. Ferfera-Harrar H, Aouaz N, Dairi N (2016) Environmental-sensitive chitosan-gpolyacrylamide/carboxymethylcellulose superabsorbent composites for wastewater purification I: synthesis and properties. *Polym Bull* 73:815–840. doi:10.1007/s00289-015-1521-2